Environmental Pollution 372 (2025) 126050

Contents lists available at ScienceDirect

Environmental Pollution

journal homepage: www.elsevier.com/locate/envpol

Multiomics analysis revealed the effects of polystyrene nanoplastics at different environmentally relevant concentrations on intestinal homeostasis☆

Jian-Zheng Yang [a], Ji-Hui Li [a], Jia-Li Liu [a], An-Ding Zhou [a], Hui Wang [b], Xiao-Li Xie [c], Kai-Kai Zhang [a,*], Qi Wang [a,**]

[a] Guangzhou Key Laboratory of Forensic Multi-Omics for Precision Identification, School of Forensic Medicine, Southern Medical University, Guangzhou, Guangdong, 510515, China
[b] Department of Pediatric Surgery, Guangzhou Women and Children's Medical Center, Guangzhou Medical University, National Children's Medical Center for South Central Region, Guangzhou, 510623, China
[c] Department of Toxicology, School of Public Health, Southern Medical University (Guangdong Provincial Key Laboratory of Tropical Disease Research), Guangzhou, Guangdong, 510515, China

ARTICLE INFO

Keywords:
Polystyrene nanoplastics
Intestinal homeostasis
Gut microbiota
Histidine metabolism
Inflammatory signaling pathway

ABSTRACT

Nanoplastics pollution is a global issue, with the digestive tract being one of the first affected organs, requiring further research on its impact on intestinal health. This study involved orally exposing mice to polystyrene nanoplastics (PS-NPs) at doses of 0.1, 0.5, or 2.5 mg/d for 42 days. The effects on intestinal health were thoroughly assessed via microbiomics, metabolomics, transcriptomics, and molecular biology. Our study demonstrated that the administration of all three doses of PS-NPs resulted in increased colonic permeability, heightened colonic and peripheral inflammation, reduced levels of antimicrobial peptides, and shortened colonic length. These effects may be attributed to a reduction in the abundance of probiotic bacteria, such as Clostridia_UCG-014, Roseburia, and Akkermansia, alongside an increase in the abundance of the pathogenic bacterium Desulfovibrionaceae induced by PS-NPs. Furthermore, we underscored the crucial role of histidine metabolism in PS-NPs-induced colonic injury, characterized by a significant reduction of L-histidine, which is closely related to microbial ecological dysregulation. Corresponding to microbiota deterioration and metabolic dysregulation, transcriptome analysis revealed that PS-NPs may disrupt colonic immune homeostasis by activating the TLR4/MyD88/NF-κB/NLRP3 signaling pathway. In conclusion, this study provided novel insights into the mechanisms by which PS-NPs disrupt intestinal homeostasis through integrated multiomics analysis, revealing critical molecular pathway and providing a scientific basis for future risk assessment of nanoplastics exposure.

1. Introduction

Statistical evidence indicates that global plastic waste generation has surpassed 400 million tons (Tejaswini et al., 2022). Over time, these plastic products degrade into microplastics and nanoplastics (NPs) (Galloway et al., 2017). A previous study indicated that microplastics in the environment further fragment into NPs, resulting in a significant increase in their quantity (Wagner and Reemtsma, 2019). The persistence of plastics has led to their pervasive presence in the environment, constituting a global pollution issue (Gigault et al., 2018). Moreover, as increasing evidence has revealed their widespread presence in various human organs, concerns have been raised regarding their potential toxicity (Leslie et al., 2022; Schwabl et al., 2019; Zhong et al., 2024).

Oral exposure constitutes a primary pathway for the ingestion of plastic particles in humans (Prata et al., 2020). Research in animals has demonstrated that post-ingestion, these particles accumulate in the liver, kidneys and intestines, with the intestinal tissue exhibiting the highest concentrations (Deng et al., 2017). Recent advances in intestinal toxicity studies of NPs have focused predominantly on single-dose exposure and lack corresponding sequencing data (Liang et al., 2021;

☆ This paper has been recommended for acceptance by Maria Cristina Fossi.
* Corresponding author.
** Corresponding author.
E-mail addresses: 304470379@qq.com (K.-K. Zhang), wangqi1980@smu.edu.cn (Q. Wang).

https://doi.org/10.1016/j.envpol.2025.126050
Received 25 November 2024; Received in revised form 16 February 2025; Accepted 11 March 2025
Available online 12 March 2025

Xu et al., 2023). Moreover, a previous literature review emphasized a notable deficiency in the application of multiomics approaches despite the considerable volume of ongoing research in this field (Das, 2023). Consequently, we integrated the microbiome, metabolome and transcriptome to reveal the potential mechanisms through which PS-NPs induce disruptions in intestinal homeostasis across various environmentally relevant concentrations.

Gut homeostasis is primarily a dynamic equilibrium involving interactions among the gut microbiota, the host mucosal barrier, metabolites and intestinal immunomodulation (Patel and Stappenbeck, 2013; Peterson and Artis, 2014; Turner, 2009). Disruptions of intestinal homeostasis can influence the pathogenesis of diseases in distal organs via the enterohepatic (Zhang et al., 2023a), enteroencephalic (Yang et al., 2023; Zhang et al., 2023b), and enteropulmonary (Dang and Marsland, 2019) axes. Therefore, a comprehensive investigation into the impact of PS-NPs on intestinal homeostasis will contribute to the future understanding of distal organ toxicity.

In this study, we investigated the effects of environmentally relevant dosages of PS-NPs on intestinal homeostasis in a mouse model. Our approach integrated multiomics analysis to systematically examine the potential mechanisms underlying PS-NPs-induced intestinal dysfunction and evaluate associated health risks.

2. Materials and methods

2.1. Chemicals and antibodies

We purchased nonfunctional PS-NPs from Tesulang Chemical Materials Co., Ltd., located in Dongguan, with a particle diameter of 100 nm and a purity exceeding 99 %. The morphological characteristics of the NPs were examined by scanning electron microscopy (SEM) (SU8010, Hitachi, Japan), and their size distribution was assessed via a particle sizing instrument (Zetasizer NANOZS, Malvern, UK). A range of antibodies were employed for this study, including anti-Occludin (Proteintech, Cat #: 13409-1-AP, ratio: 1:2000), anti-Claudin5 (ABclonal, Cat #: A25830, ratio: 1:2000), anti-TLR4 (Santa Cruz, Cat #: sc-13591, ratio: 1:1000), anti-MyD88 (CST, Cat #: 4283S, ratio: 1:1000), anti-phospho-NF-κB (Ser536) (Abmart, Cat #: TP56372S, ratio: 1:1000), anti-NF-κB (CST, Cat #: 8242S, ratio: 1:1000), anti-NLRP3 (Abcepta, Cat #: AP8564A, ratio: 1:1000), anti-IL-1β (Affinity, Cat #: AF4006, ratio: 1:1000), and anti-β-actin (Proteintech, Cat #: 20536-1-AP, ratio: 1:5000).

2.2. Polystyrene nanoplastics (PS-NPs) administration

To comprehensively evaluate the impact of NPs on colon and serum metabolism, doses of 0.1, 0.5, and 2.5 mg/day were selected for this study. Specifically, thirty-two male C57BL/6 mice were randomly allocated into four experimental groups, each consisting of eight individuals: a control group (Con) receiving 0.2 mL of sterile Milli-Q water via oral gavage and three treatment groups receiving 0.2 mL of NPs suspensions at concentrations of 0.5 mg/mL (low dose, LD), 2.5 mg/mL (medium dose, MD), and 12.5 mg/mL (high dose, HD), respectively. Daily gavage administration was conducted for a duration of six consecutive weeks.

2.3. Tissue collection

Fecal samples were collected for 16S rRNA sequencing within 12 h after the last treatment. Next, we anesthetized the mice and collected blood via cardiac puncture. Blood serum was extracted by spinning the samples at 4 °C with a centrifugal force of 4000×*g* for a duration of 10 min. Meanwhile, the colonic tissue samples were preserved either in a 4 % paraformaldehyde solution or at -80 °C for further analysis.

2.4. Serum biochemical analysis

Following the guidelines provided by Jiangsu Meimian Industrial Co., Ltd., we employed an enzyme-linked immunosorbent assay (ELISA) to quantify lipopolysaccharide (LPS, Cat #: MM-0634M2).

2.5. Measurement of inflammatory cytokines

Three kits were used (Jiangsu Meibiao Biotechnology Co., Ltd.): tumor necrosis factor-alpha (TNF-α; MB-2868B), interleukin-6 (IL-6; MB-2899B), and interleukin-1 beta (IL-1β; MB-2776B).

A full description of the materials and methods is given in the Supplementary Material.

3. Results

3.1. Characterization of PS-NPs and their effects on body weight and colon length in mice

Physical property analysis revealed that the PS-NPs exhibited a uniform spherical morphology with an average diameter of 113.3 nm (Fig. 1A and B). In this study, the mice were orally administered NPs or an equal volume of vehicle for 42 consecutive days to induce colonic injury (Fig. 1C). We first observed that after six weeks of continuous exposure to the LD, MD and HD PS-NPs, the mice gradually gained weight, with no difference compared with those in the Con group (Fig. 1D). However, a significant reduction in colon length was observed in the PS-NPs-exposed groups compared to the Con group (Fig. 1E).

3.2. Exposure to PS-NPs disrupted intestinal barrier function in mice

To investigate the effects of PS-NPs on intestinal barrier function, we performed histological and molecular analyses. H&E staining revealed that exposure to PS-NPs led to inflammatory cell infiltration within the colonic mucosa (Fig. 2A). PAS and AB staining revealed a significant decrease in the number of PAS^{+} and AB^{+} goblet cells in the PS-NPs-exposed groups compared with the Con group, suggesting impaired mucus production (Fig. 2B and C). In addition, increased serum levels of LPS suggested that PS-NPs treatment contributed to impaired intestinal barrier function (Fig. 2D). This finding was also confirmed by decreased mRNA and protein expression of tight junction proteins (Fig. 2E and F). Furthermore, PS-NPs treatment downregulated the expression of *Il-23*, *Il-22*, and *Reg3γ* (Fig. 2G), genes involved in the IL-23/IL-22/Reg3γ signaling pathway known to regulate antimicrobial peptide production. Increased intestinal permeability facilitates the translocation of macromolecules, including bacteria and toxins, across the intestinal mucosa, thereby initiating peripheral inflammation. Subsequent analysis of inflammatory markers in the peripheral serum revealed that PS-NPs exposure significantly elevated the serum levels of the pro-inflammatory cytokines IL-6 and IL-1β (Fig. 2H). These results collectively indicated that chronic exposure to environmentally relevant concentrations of PS-NPs, even at low doses, disrupted intestinal barrier function and promoted systemic inflammation.

3.3. PS-NPs disrupted the gut microbial composition in mice

Gut barrier integrity and gut microbes are important components of gut homeostasis. To further understand the impact of the three doses of PS-NPs on the gut microbial composition, we conducted 16S rRNA sequencing analysis. Alpha diversity, as measured by the ace, chao, shannon, and simpson indices, revealed a significant reduction in bacterial richness and diversity in the HD PS-NPs group compared with the Con group (Fig. 3A and B). A Venn diagram of the observed OTUs demonstrated a dose-dependent decrease in the number of OTUs following PS-NPs exposure (Fig. 3C). For beta diversity, both principal coordinate analysis (PCoA, $R = 0.2395$, $P = 0.004$) and PLS-DA revealed

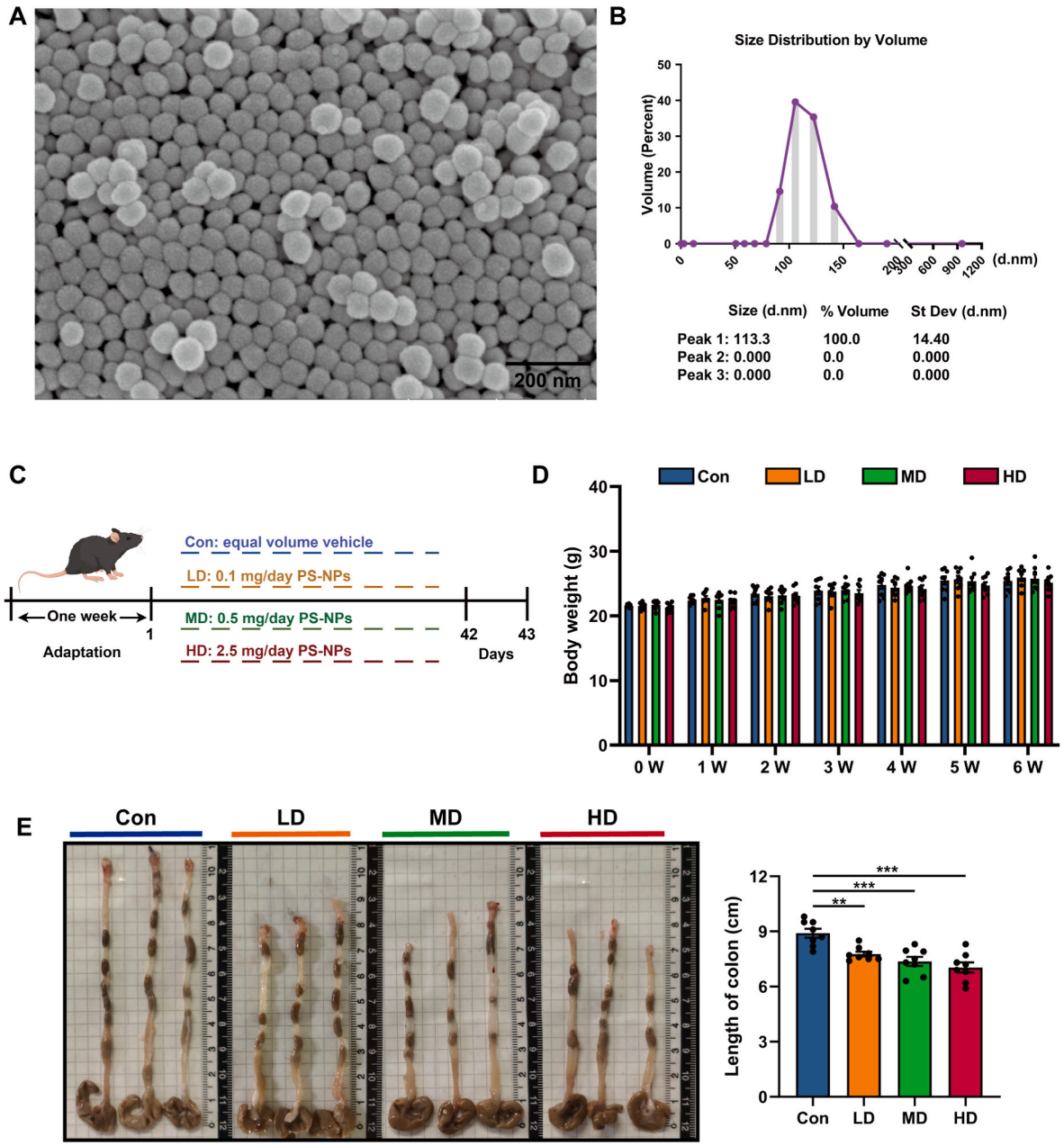

Fig. 1. PS-NPs shorten the colon length in mice. Characterization of PS-NPs (A) morphology and (B) particle size. (C) Experimental flow chart. (D) Weight monitoring after continuous administration. (E) Representative images of the colons from the four groups of mice. The data were presented as the mean ± SEM. n = 8 per group. One-way ANOVA with Tukey's multiple comparisons test was used. **: $p < 0.01$, ***: $p < 0.001$ versus the Con group.

distinct clustering patterns between the Con- and PS-NPs-exposed groups (Fig. 3D and E). In terms of the bacterial characterization index, the PS-NPs groups presented a significantly higher microbial dysbiosis index (MDI) and a significantly lower gut microbial health index (GMHI) compared to the Con group (Fig. 3F and G). At the phylum level, Bacteroidetes and Firmicutes dominated across all groups (Fig. 3H). The relative abundances of the top 20 most abundant genera are presented in Fig. 3I. To observe the effects of PS-NPs on the gut microbial composition, we selected 8 representative taxa among all the genera. The abundances of Clostridia_UCG-014, Tuzzerella, Roseburia and Akkermansia were dramatically lower in the PS-NPs group than in the Con group (Fig. 3J). Conversely, the abundances of Lachnospiraceae_NK4A136_group, Parabacteroides, Anaerofustis and Desulfovibrionaceae significantly increased after PS-NPs treatment (Fig. 3K).

Spearman correlation analysis was subsequently used to elucidate the potential relationships between the gut microbiota and both colonic injury and peripheral inflammation. The findings indicated that the probiotic bacteria Clostridia_UCG-014, Roseburia and Akkermansia were positively correlated with colonic indices, including colon length and the counts of PAS^+ and AB^+ goblet cells. Conversely, the potentially pathogenic bacterium Desulfovibrionaceae was negatively correlated with these colonic indices. With respect to peripheral inflammation, Clostridia_UCG-014, Roseburia and Akkermansia exhibited a negative correlation with the upregulation of inflammatory cytokines, whereas Desulfovibrionaceae was positively correlated with these cytokines (Fig. 3L). These correlation results suggested a potential role for gut microbiota dysbiosis in mediating PS-NPs-induced colonic injury and systemic inflammation.

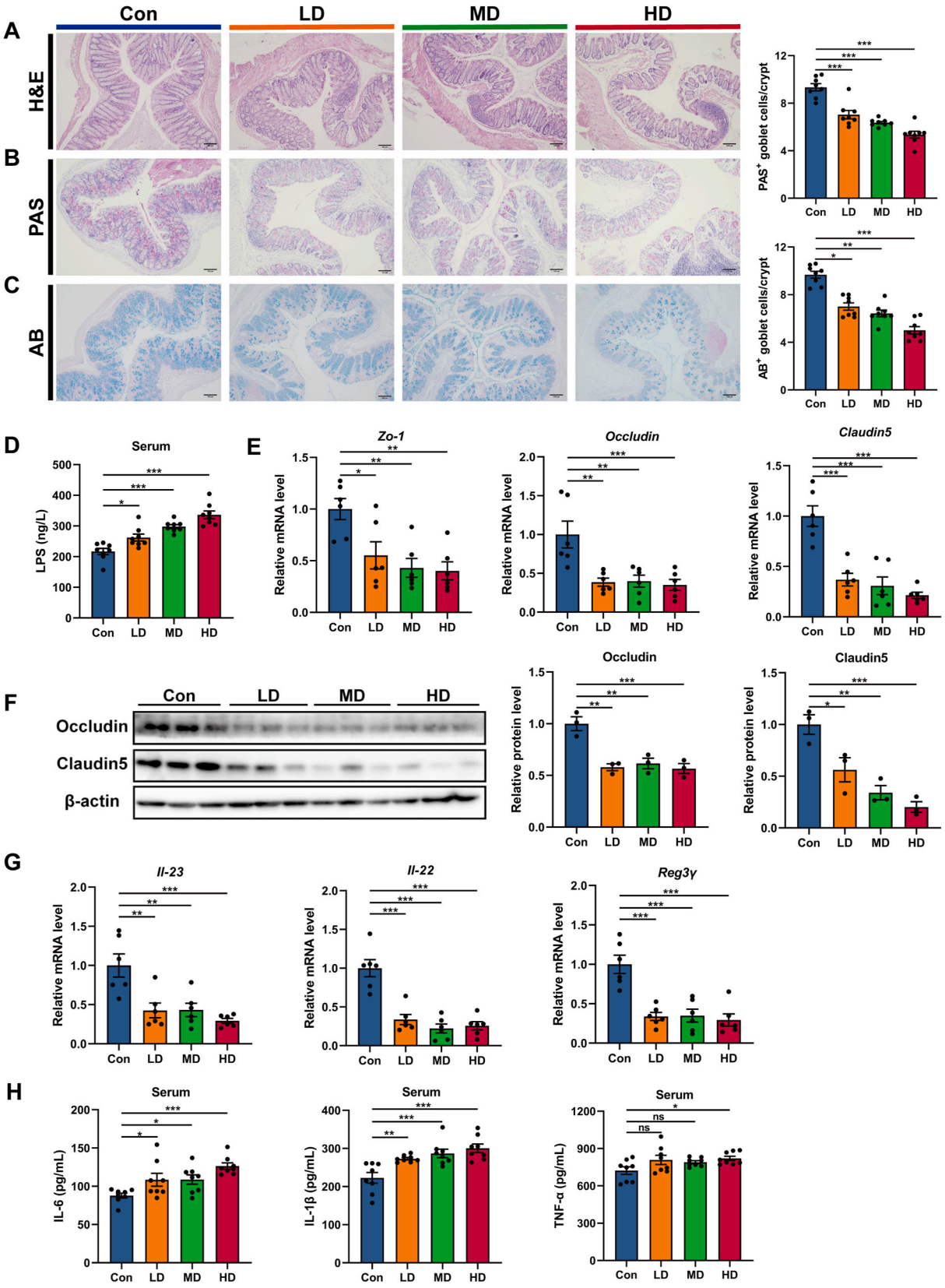

Fig. 2. PS-NPs increased intestinal permeability. Representative images of (A) H&E, (B) PAS and (C) AB staining of colonic tissue sections from different groups of mice. (D) Serum levels of LPS. (E) Relative expression of the tight junction-related mRNAs *Zo-1*, *Occludin* and *Claudin-5* across the groups. (F) The protein expression of occludin, claudin-5 and β-actin was analyzed via WB. (G) The relative mRNA expression levels of *Il-23*, *Il-22* and *Reg3γ* in the colonic mucosa. (H) Serum levels of the pro-inflammatory cytokines IL-6, IL-1β and TNF-α across the groups. The data were presented as the mean ± SEM. n = 3–8 per group. One-way ANOVA with Tukey's multiple comparisons or the Kruskal–Wallis test followed by Dunn's post hoc test were used. *: $p < 0.05$, **: $p < 0.01$, ***: $p < 0.001$ versus the Con group.

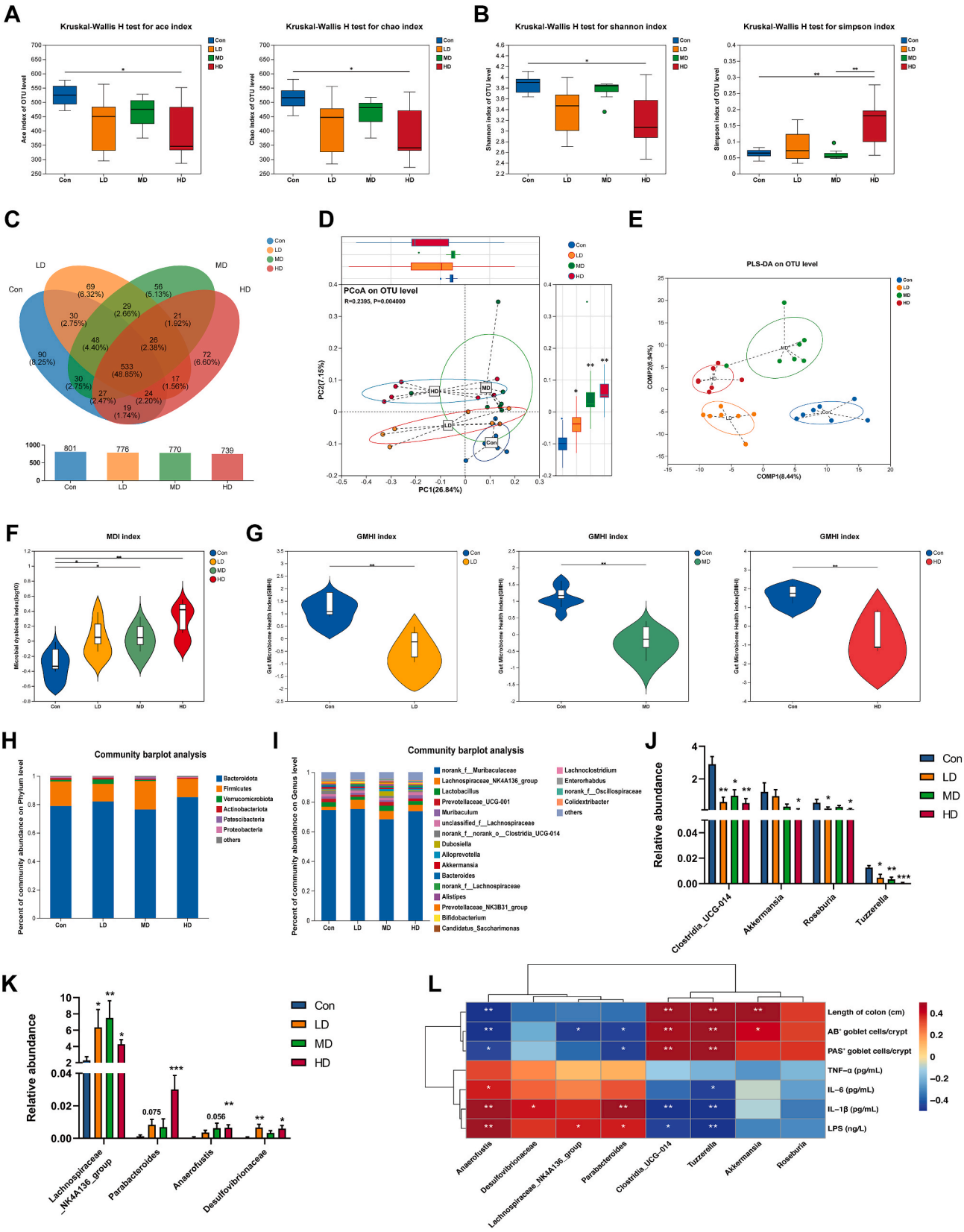

Fig. 3. PS-NPs induced gut microbiota dysbiosis. (A–B) The ace, chao, shannon and simpson indices were used to represent alpha diversity. (C) Venn diagram analysis of the Con, LD, MD and HD groups. (D–E) PCoA and PLS-DA analysis at the OTU level. (F–G) PS-NPs treatment increased the MDI and decreased the GMHI. Community bar plot analysis at the (H) phylum and (I) genus levels. (J–K) The relative abundance of 8 representative bacterial genera. (L) Spearman correlation analysis. The data were presented as the mean ± SEM. n = 7 per group. The Wilcoxon rank-sum test and Kruskal–Wallis test were used. *: $p < 0.05$, **: $p < 0.01$, ***: $p < 0.001$ versus the Con group.

3.4. PS-NPs restructured gut microbial metabolites

To elucidate the metabolic profile of the gut microbiota potentially involved in PS-NPs-induced colonic injury, we conducted an untargeted metabolomic analysis of serum samples. PLS-DA demonstrated significant differences in serum metabolites between the PS-NPs-exposed groups and the Con group, with the permutation test confirming the robustness of the PLS-DA model (Fig. 4A and B). A total of 348, 345, and 522 differentially abundant metabolites (VIP >1, $p < 0.05$) were identified in the LD, MD, and HD PS-NPs groups, respectively, compared to the Con group. Subsequent KEGG analysis revealed that all the significantly enriched pathways were predominantly associated with amino acid metabolism. Further examination of the top five pathways indicated that the histidine metabolism pathway was significantly enriched across all three doses of PS-NPs (Fig. 4C-E). The heatmap revealed specific metabolite changes, highlighting the significant downregulation of L-histidine, which is known for its anti-inflammatory properties, in the PS-NPs groups compared with the Con group (Fig. 4F). Spearman's correlation analysis revealed that L-histidine was positively correlated with the colonic indices and negatively correlated with the upregulation of inflammatory cytokines (Fig. 4G). Furthermore, the probiotics Clostridia_UCG-014, Roseburia, and Akkermansia were significantly positively correlated with the L-histidine levels, whereas Desulfovibrionaceae was negatively correlated with the L-histidine levels (Fig. 4H). These correlation analyses suggested the association between the gut microbiota and its metabolites in PS-NPs-induced injury, suggesting the critical role of histidine metabolism.

3.5. PS-NPs altered the transcriptomic profile of the mice colon

To better understand the molecular mechanisms of PS-NPs-induced colon-related pathology, we conducted mRNA sequencing. Principal component analysis (PCA) revealed that exposure to PS-NPs resulted in altered colonic gene expression, compared with the Con group, especially in the MD and HD groups (Fig. 5A). The volcano plot revealed that, compared with Con, exposure to LD, MD and HD PS-NPs resulted in 2,011, 1,654, and 3686 DEGs, respectively (Fig. 5B). Among these genes, 247 genes were coregulated (Fig. 5C). Heatmap analysis revealed that the majority of these coregulated genes were upregulated, with a pattern suggesting dose-dependent effects (Fig. 5D). KEGG annotation analysis revealed that 'signaling transduction' and 'signaling molecules and interaction' were significantly enriched (Fig. 5E). We further conducted KEGG enrichment analysis on the DEGs across the three groups. The analysis highlighted the involvement of inflammatory pathways, including 'TNF signaling', 'NF-kappa B signaling', 'Toll-like receptor signaling', 'NOD-like receptor signaling' and 'inflammatory bowel disease' (Fig. 5F–H). In summary, the transcriptomic results suggested that PS-NPs-induced intestinal injury is associated with inflammatory activation.

3.6. PS-NPs induced colonic inflammation via activation of the TLR4/MyD88/NF-κB/NLRP3 signaling pathway

The TLR4/MyD88/NF-κB/NLRP3 signaling pathway has been implicated in various inflammatory processes, including neuroinflammation (Sun et al., 2023), cardiomyocyte pyroptosis (Chen et al., 2022), and LPS-stimulated inflammatory responses (Zhang et al., 2022). In conjunction with the findings from RNA-seq, to assess the involvement of this pathway in PS-NPs-mediated colonic inflammation, we examined the expression of key pathway components. WB analysis revealed that PS-NPs treatment significantly increased the expression of TLR4, MyD88, NLRP3 and IL-1β and increased the phospho-NF-κB/NF-κB ratio compared with Con treatment (Fig. 6A). Furthermore, PS-NPs treatment significantly upregulated the mRNA expression of pro-inflammatory cytokines *Il-1β*, *Il-6* and *Tnf-α* in colonic tissue (Fig. 6B). These data suggested that activation of the TLR4/MyD88/NF-κB/NLRP3 pathway contributes to PS-NPs-induced colonic inflammation.

4. Discussion

With the accumulation of increasing amounts of micro- and nanoplastics in the environment, their potential impact on human health deserves more comprehensive study. Human exposure to plastic particles is estimated to range from 0.23 to 11.9 mg/kg per day (Senathirajah et al., 2021). A previous publication indicated that human and mouse body surface areas are 1.62 and 0.007 square meters, respectively, and body weights are 60 and 0.02 kg, respectively; thus, the exposure dose conversion formula for humans and mice on the basis of body surface area yields an equivalent dose of 0.05–2.9 mg/day for 0.02 kg mice (Nair and Jacob, 2016; Xu et al., 2023; Yang et al., 2024). We therefore exposed mice to human equivalent doses of PS-NPs to explore their potential effects on the intestinal system. We reported that PS-NPs inhibited the hyperplasia of colonic goblet cells, reduced mucus secretion, and decreased the expression of tight junction proteins and antimicrobial peptides, consequently leading to increased colonic permeability. Furthermore, PS-NPs exposure significantly elevated the serum LPS and pro-inflammatory cytokines (IL-6 and IL-1β) levels. These effects were significantly correlated with PS-NPs-induced disruptions in the gut microbiota composition and alterations in histidine metabolism. Additionally, our findings revealed that PS-NPs activated the TLR4/MyD88/NF-κB/NLRP3 signaling pathway, which may mediate the observed colonic inflammation (Fig. 7). These findings offer a significant understanding of the possible health risks associated with NPs exposure.

The gut microbial composition plays a critical role in maintaining intestinal homeostasis, and dysbiosis is implicated in various intestinal diseases (Lee et al., 2022; Litvak et al., 2018). Akkermansia, a pivotal bacterium for sustaining intestinal integrity, has been implicated in the progression of inflammatory bowel disease (Paone and Cani, 2020; Wu et al., 2021). Elevated Clostridia_UCG-014 levels have been shown to mitigate colitis and mucosal damage (Gong et al., 2024; Y. He et al., 2022). Furthermore, Roseburia is a probiotic that contributes to alleviating colon inflammation and plays a regulatory role in maintaining the intestinal barrier and modulating cytokine release (Kang et al., 2023; Nie et al., 2021). A previous study reported notable enrichment of Desulfovibrionaceae in individuals with ulcerative colitis, contributing to the exacerbation of this condition (Xie et al., 2024). In the present investigation, we observed that exposure to PS-NPs resulted in a reduction in Clostridia_UCG-014, Roseburia and Akkermansia, coupled with an increase in the pathogenic bacterium Desulfovibrionaceae. These alterations in the gut microbial composition may underlie the colonic injury and peripheral inflammation induced by PS-NPs.

The gut microbiota can influence host function through its metabolites (Gao et al., 2017). It has been shown that Akkermansia significantly upregulates histidine levels in modified brain–heart infusion medium (Zhang et al., 2024). Furthermore, the modulatory effect of Pi-Dan-Jian-Qing decoction on serum histidine is associated with an altered abundance of Akkermansia (Xie et al., 2021). Bioactive peptides exhibited protective effects in a mouse cerebral infarction model by highly enriching Roseburia and upregulating histidine (Ji et al., 2024). Clostridia_UCG-014 also had a significant positive correlation with histidine in concentrate-supplemented large animals (Yi et al., 2023). In the present study, with the disruption of the gut microbial composition described above, PS-NPs substantially impacted histidine metabolism, which was characterized mainly by a consistent reduction in L-histidine levels across various doses of PS-NPs.

Histidine is an essential amino acid that plays a crucial role as a ROS scavenger and an anti-inflammatory mediator (Holeček, 2020; Son et al., 2005). Notably, significant decreases in serum histidine levels have been observed in multiple population-based cohorts of patients with inflammatory bowel disease (IBD), potentially indicating chronic

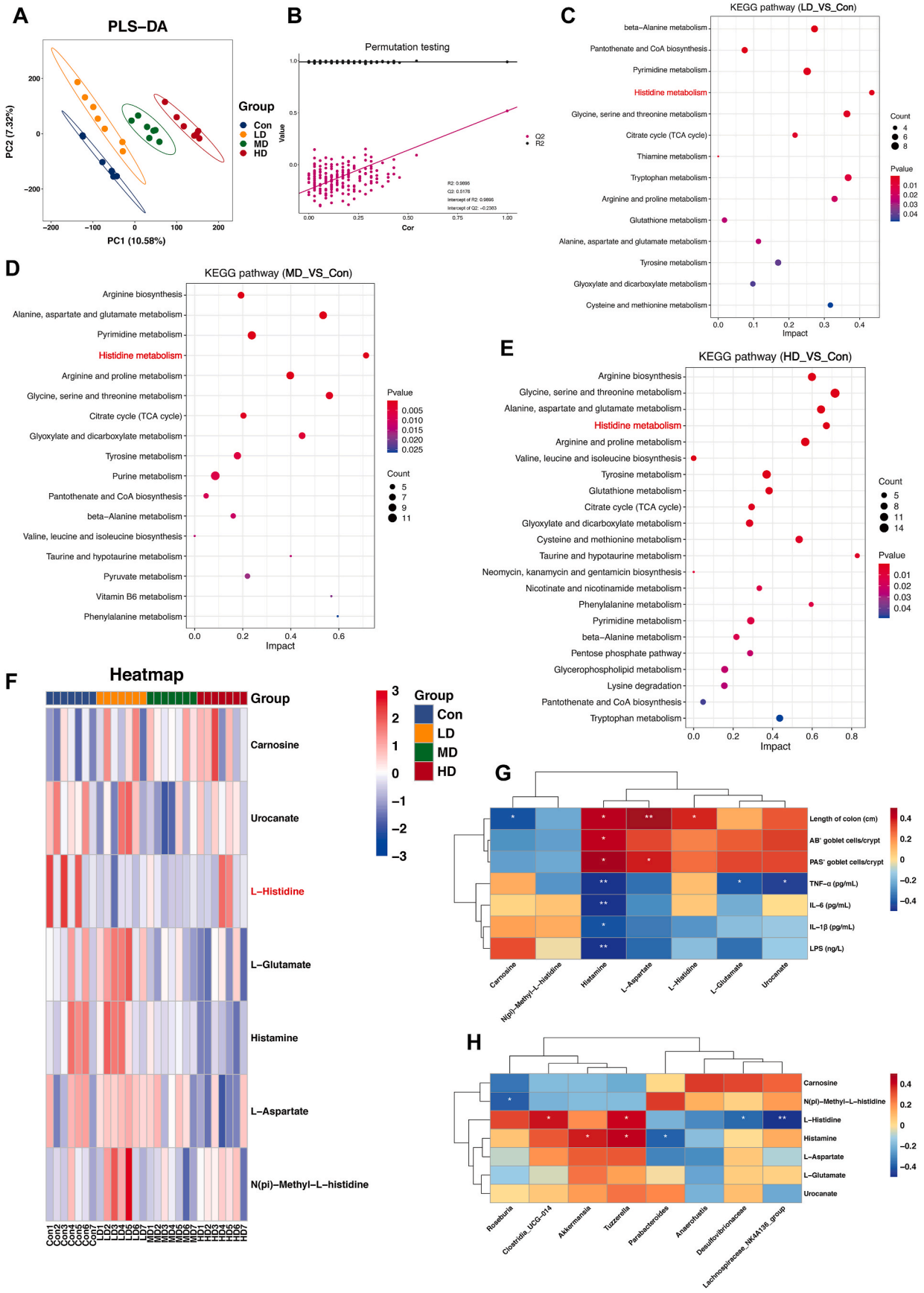

Fig. 4. PS-NPs significantly altered the histidine metabolic pathway in the serum. (A–B) PLS-DA analysis and corresponding permutation testing revealed significant metabolite changes between the PS-NPs and Con groups. (C–E) KEGG pathway analysis of differentially abundant metabolites across groups. (F) Heatmap showing the levels of metabolites enriched in histidine metabolism. (G–H) Spearman correlation analysis. n = 7 per group.

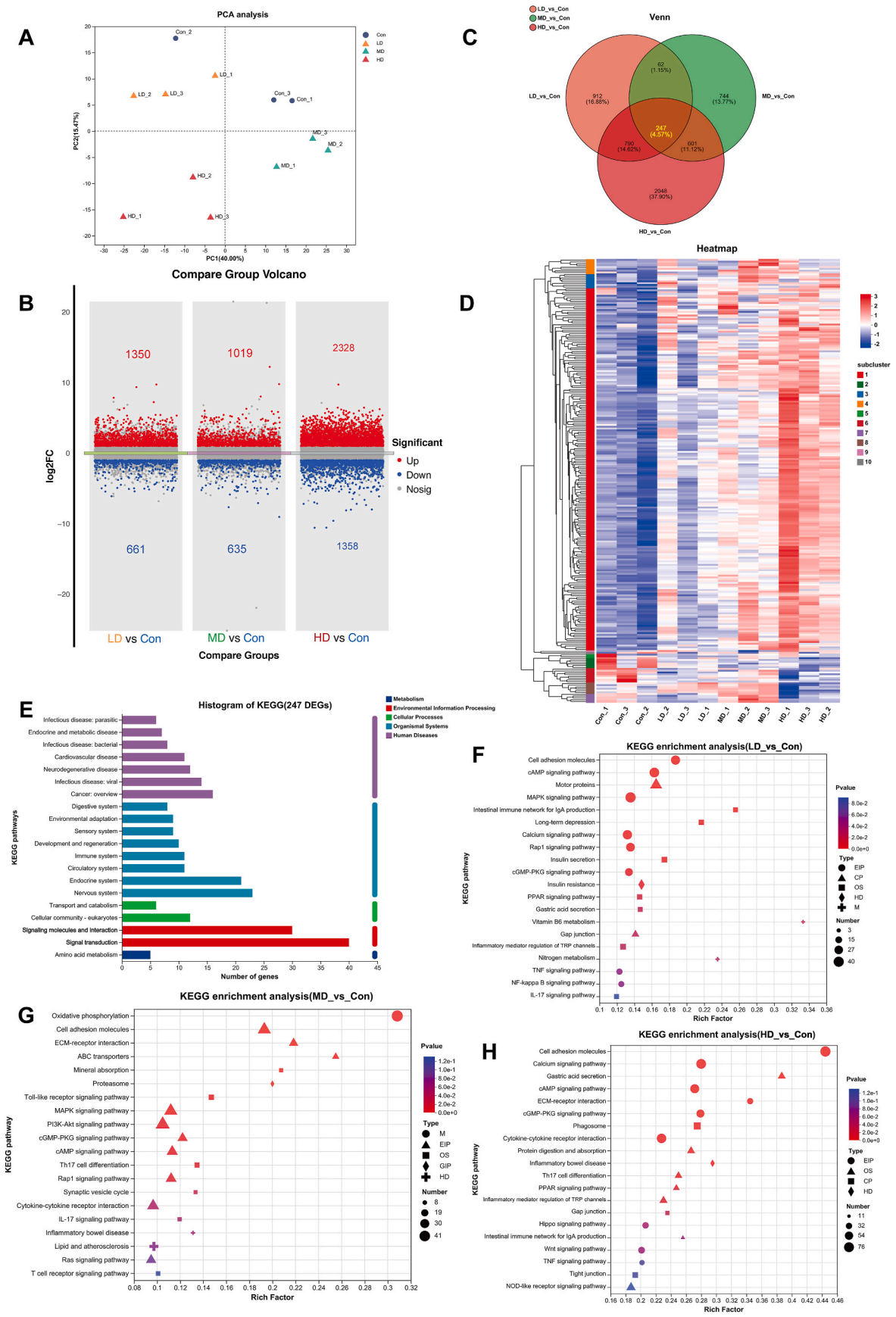

Fig. 5. PS-NPs induced alterations in pathways associated with colonic inflammation. (A) PCA was used to demonstrate the clustering of samples. (B) Compare group volcano plots to show DEGs. (C) Venn diagram analysis of the Con, LD, MD and HD groups. (D) Heatmap of the 247 DEGs. (E) Annotation analysis of 247 DEGs. (F–H) Plots of the results of the KEGG enrichment analysis of DEGs among different groups. n = 3 per group.

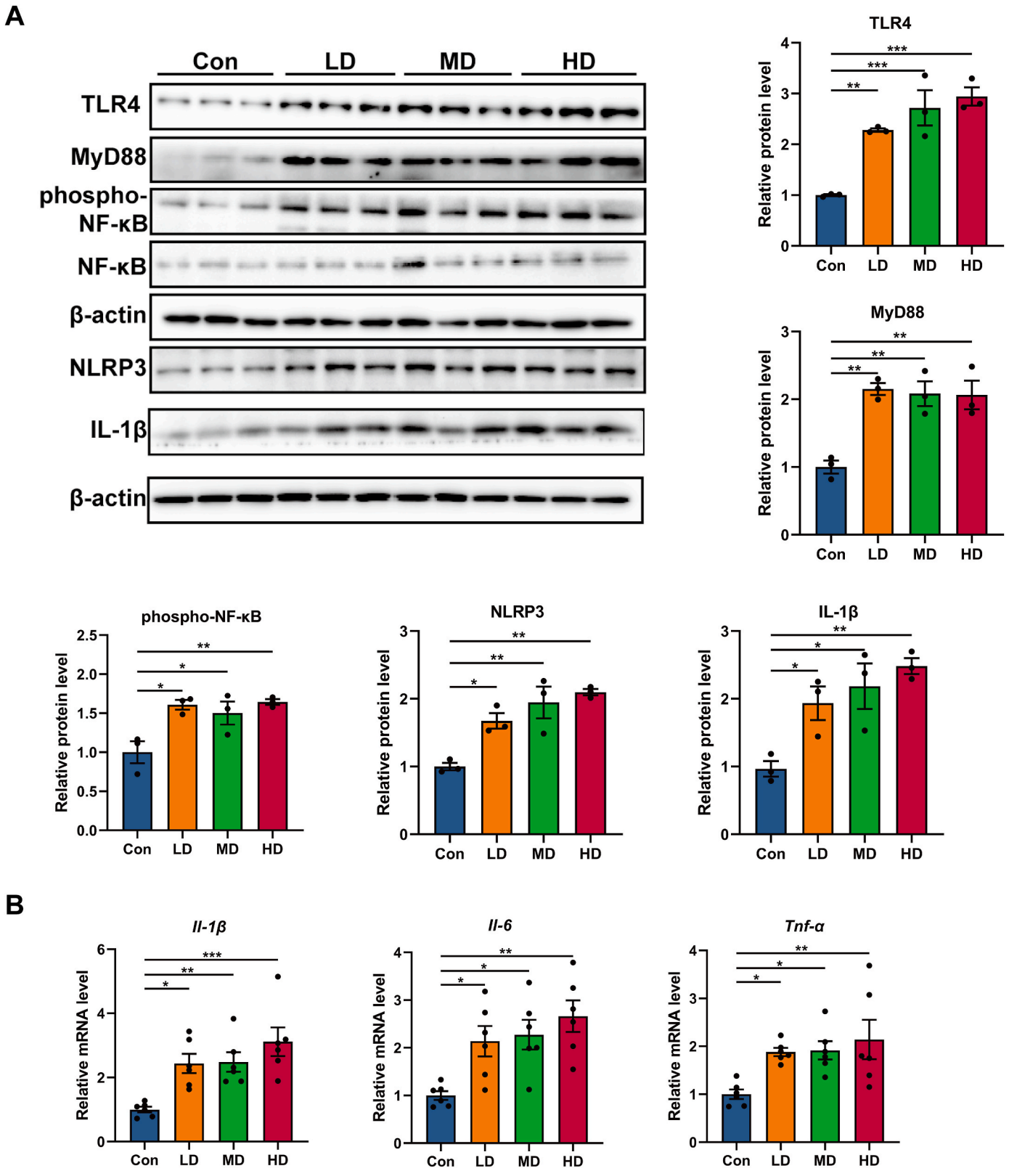

Fig. 6. Validation of the TLR4/MyD88/NF-κB/NLRP3 signaling pathway. (A) The expression of the proteins TLR4, MyD88, phospho-NF-κB, NF-κB, NLRP3, IL-1β and β-actin was analyzed via WB. (B) Relative mRNA expression levels of the pro-inflammatory cytokines *Il-1β*, *Il-6* and *Tnf-α* in the colonic mucosa. The data were presented as the mean ± SEM. n = 3–6 per group. One-way ANOVA with Tukey's multiple comparisons test was used. *: $p < 0.05$, **: $p < 0.01$, ***: $p < 0.001$ versus the Con group.

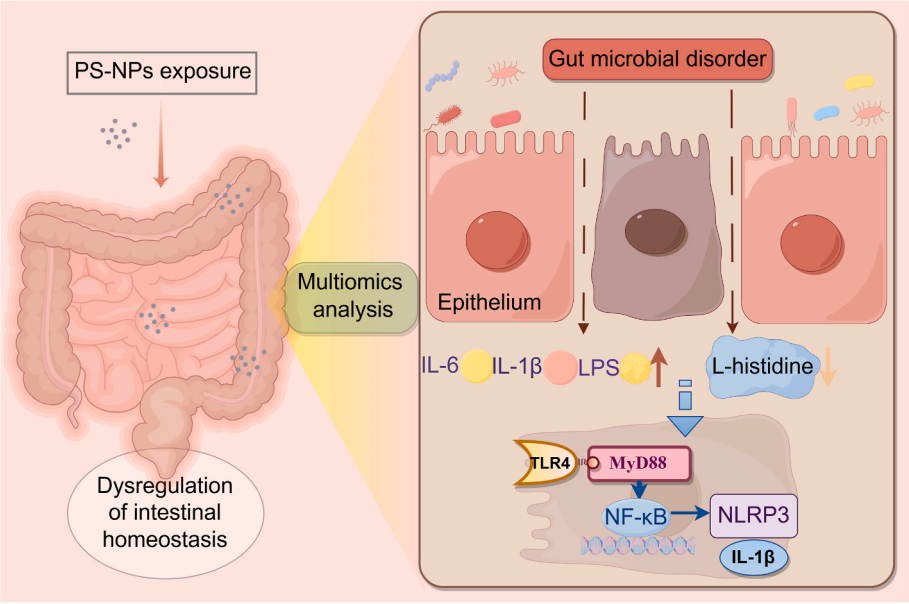

Fig. 7. Mechanistic model diagram of the present study. Extended exposure to human-equivalent doses of nanoplastics results in the disruption of intestinal homeostasis. This phenomenon is attributed to alterations in the gut microbial composition, which subsequently leads to a reduction in the circulating levels of microbial-derived L-histidine and an increase in the levels of inflammatory factors. These changes ultimately activate inflammatory signaling pathways within the colonic tissue.

inflammation in these individuals (Hisamatsu et al., 2012; Kohashi et al., 2014; Probert et al., 2018). Research has indicated that histidine metabolism plays a role in copper-induced intestinal barrier dysfunction and inflammation (Liao et al., 2021). Fructose has been shown to exacerbate colitis by reducing histidine levels (Song et al., 2023). Whereas enteral nutrition has been shown to alleviate colitis through gut microbial-mediated histidine biosynthesis (Zeng et al., 2024). Previous in vitro experiments and animal models have shown that lower levels of histidine do not effectively inhibit NF-κB, leading to increased LPS-induced inflammation (Andou et al., 2009; Cortes et al., 2022; Hasegawa et al., 2011), whereas exogenous supplementation with histidine can ameliorate LPS-induced inflammation by inhibiting the activation of the NLPR3 inflammasome. Our sequencing and WB results revealed that PS-NPs induced activation of the TLR4/MyD88/NF-κB/NLRP3 pathway. Consequently, we propose that the observed reduction in histidine levels contributes to PS-NPs-mediated colonic inflammation and barrier dysfunction via this signaling cascade. Similarly, He et al. reported that PS-NPs worsened duodenal permeability and inflammatory responses in mice through the NF-κB/NLRP3 pathway (Z. He et al., 2022), and Chen et al. reported that PS-NPs induced intestinal and hepatic inflammation through activation of the NF-kappaB/NLRP3 pathway (Chen et al., 2024). Taken together, these findings suggest that NLRP3 is deeply involved in PS-NPs induced toxicity.

However, from the perspective of therapeutic target discovery, whether exogenous supplementation with histidine and inhibitors of NLRP3 are protective against PS-NPs-induced colonic inflammation and injury deserves further exploration. The exploration of the effectiveness of these potential therapeutic targets will be the direction of our future research. The main findings of this study were that exposure to different human equivalent doses of PS-NPs led to alterations in gut microbes, which in turn led to a decrease in histidine and activation of the TLR4/MyD88/NF-κB/NLRP3 pathway in the colon. Our research will help raise attention to the intestinal health problems caused by nanoplastics and increase people's awareness of the need for prevention.

Furthermore, several limitations of this study should be acknowledged. Future investigations should incorporate comprehensive biodistribution analyses to assess PS-NPs accumulation in internal organs. Additionally, study designs should be expanded to include larger animal cohorts, both genders, extended exposure durations, and diverse nanoplastic types to enhance the generalizability and translational relevance of the findings. Fecal microbial transplantation experiments are essential to validate the contribution of the gut microbiota in the next step of the study.

5. Conclusion

In summary, this study integrated microbiomics, metabolomics and transcriptomics to investigate the impact of PS-NPs on critical components of intestinal homeostasis, including the intestinal barrier, gut microbial composition, microbial metabolism and colonic immune responses. Our findings demonstrated that PS-NPs disrupt intestinal homeostasis by altering the gut microbiota, suppressing histidine synthesis and activating the TLR4/MyD88/NF-κB/NLRP3 signaling pathway.

CRediT authorship contribution statement

Jian-Zheng Yang: Writing – original draft, Methodology, Investigation. **Ji-Hui Li:** Project administration. **Jia-Li Liu:** Project administration. **An-Ding Zhou:** Formal analysis. **Hui Wang:** Formal analysis. **Xiao-Li Xie:** Funding acquisition, Conceptualization. **Kai-Kai Zhang:** Writing – review & editing, Funding acquisition. **Qi Wang:** Writing – review & editing, Supervision, Funding acquisition.

Funding

This work was supported by the National Natural Science Foundation of China (Grant Nos. 82171877, 82173474, 82471914 and 82400701) and the Guangdong Basic and Applied Basic Research Foundation (Grant Nos. 2023A1515012476 and 2024A1515010708).

Declaration of competing interest

The authors declare that they have no known competing financial interests or personal relationships that could have appeared to influence the work reported in this paper.

Acknowledgment

The graphical abstract and flowchart were drawn by Figdraw (www.home-for-researchers.com). During the preparation of this work, the authors used Home for Researchers and American Journal Experts' AI writing assistant, Rubriq (https://china.aje.com/cn/rubriq), for English language editing. After using these services, the authors reviewed and edited the content as needed and take full responsibility for the content of the publication.

Appendix A. Supplementary data

Supplementary data to this article can be found online at https://doi.org/10.1016/j.envpol.2025.126050.

Data availability

Data will be made available on request.

References

Andou, A., et al., 2009. Dietary histidine ameliorates murine colitis by inhibition of proinflammatory cytokine production from macrophages. Gastroenterology 136, 564-74.e2.
Chen, X., et al., 2022. Trimetazidine affects pyroptosis by targeting GSDMD in myocardial ischemia/reperfusion injury. Inflamm. Res. 71, 227–241.
Chen, X., et al., 2024. Polystyrene nanoplastics induce intestinal and hepatic inflammation through activation of NF-κB/NLRP3 pathways and related gut-liver axis in mice. Sci. Total Environ. 935, 173458.
Cortes, G.M., et al., 2022. Inflammatory bowel disease and COVID-19: How microbiomics and metabolomics depict two sides of the same coin. Front. Microbiol. 13, 856165.
Dang, A.T., Marsland, B.J., 2019. Microbes, metabolites, and the gut-lung axis. Mucosal Immunol. 12, 843–850.
Das, A., 2023. The emerging role of microplastics in systemic toxicity: involvement of reactive oxygen species (ROS). Sci. Total Environ. 895, 165076.
Deng, Y., et al., 2017. Tissue accumulation of microplastics in mice and biomarker responses suggest widespread health risks of exposure. Sci. Rep. 7, 46687.
Galloway, T.S., et al., 2017. Interactions of microplastic debris throughout the marine ecosystem. Nat Ecol Evol 1, 116.
Gao, B., et al., 2017. Sex-specific effects of organophosphate diazinon on the gut microbiome and its metabolic functions. Environ. Health Perspect. 125, 198–206.
Gigault, J., et al., 2018. Current opinion: what is a nanoplastic? Environ. Pollut. 235, 1030–1034.
Gong, H., et al., 2024. Structural characteristics of steamed Polygonatum cyrtonema polysaccharide and its bioactivity on colitis via improving the intestinal barrier and modifying the gut microbiota. Carbohydr. Polym. 327, 121669.
Hasegawa, S., et al., 2011. Amino acids exhibit anti-inflammatory effects in human monocytic leukemia cell line, THP-1 cells. Inflamm. Res. 60, 1013–1019.
He, Y., et al., 2022. Polystyrene nanoplastics deteriorate LPS-modulated duodenal permeability and inflammation in mice via ROS drived-NF-κB/NLRP3 pathway. Chemosphere 307, 135662.
He, Z., et al., 2022. Gut microbiota-derived ursodeoxycholic acid from neonatal dairy calves improves intestinal homeostasis and colitis to attenuate extended-spectrum β-lactamase-producing enteroaggregative Escherichia coli infection. Microbiome 10, 79.
Hisamatsu, T., et al., 2012. Novel, objective, multivariate biomarkers composed of plasma amino acid profiles for the diagnosis and assessment of inflammatory bowel disease. PLoS One 7, e31131.
Holeček, M., 2020. Histidine in health and disease: metabolism, physiological importance, and use as a supplement. Nutrients 12.
Ji, J., et al., 2024. Synergistic effects of tilapia head protein hydrolysate and walnut protein hydrolysate on the amelioration of cognitive impairment in mice. J. Sci. Food Agric. 104, 5419–5434.
Kang, X., et al., 2023. Roseburia intestinalis generated butyrate boosts anti-PD-1 efficacy in colorectal cancer by activating cytotoxic CD8(+) T cells. Gut 72, 2112–2122.
Kohashi, M., et al., 2014. A novel gas chromatography mass spectrometry-based serum diagnostic and assessment approach to ulcerative colitis. J Crohns Colitis 8, 1010–1021.
Lee, J., et al., 2022. The microbiome and gut homeostasis. Science 377, eabp9960.
Leslie, H.A., et al., 2022. Discovery and quantification of plastic particle pollution in human blood. Environ. Int. 163, 107199.
Liang, B., et al., 2021. Underestimated health risks: polystyrene micro- and nanoplastics jointly induce intestinal barrier dysfunction by ROS-mediated epithelial cell apoptosis. Part. Fibre Toxicol. 18, 20.
Liao, J., et al., 2021. Toxic effects of copper on the jejunum and colon of pigs: mechanisms related to gut barrier dysfunction and inflammation influenced by the gut microbiota. Food Funct. 12, 9642–9657.
Litvak, Y., et al., 2018. Colonocyte metabolism shapes the gut microbiota. Science 362.
Nair, A.B., Jacob, S., 2016. A simple practice guide for dose conversion between animals and human. J. Basic Clin. Pharm. 7, 27–31.
Nie, K., et al., 2021. Roseburia intestinalis: a beneficial gut organism from the discoveries in genus and species. Front. Cell. Infect. Microbiol. 11, 757718.
Paone, P., Cani, P.D., 2020. Mucus barrier, mucins and gut microbiota: the expected slimy partners? Gut 69, 2232–2243.
Patel, K.K., Stappenbeck, T.S., 2013. Autophagy and intestinal homeostasis. Annu. Rev. Physiol. 75, 241–262.
Peterson, L.W., Artis, D., 2014. Intestinal epithelial cells: regulators of barrier function and immune homeostasis. Nat. Rev. Immunol. 14, 141–153.
Prata, J.C., et al., 2020. Environmental exposure to microplastics: an overview on possible human health effects. Sci. Total Environ. 702, 134455.
Probert, F., et al., 2018. Plasma nuclear magnetic resonance metabolomics discriminates between high and low endoscopic activity and predicts progression in a prospective cohort of patients with ulcerative colitis. J Crohns Colitis 12, 1326–1337.
Schwabl, P., et al., 2019. Detection of various microplastics in human stool: a prospective case series. Ann. Intern. Med. 171, 453–457.
Senathirajah, K., et al., 2021. Estimation of the mass of microplastics ingested - a pivotal first step towards human health risk assessment. J. Hazard Mater. 404, 124004.
Son, D.O., et al., 2005. Histidine inhibits oxidative stress- and TNF-alpha-induced interleukin-8 secretion in intestinal epithelial cells. FEBS Lett. 579, 4671–4677.
Song, G., et al., 2023. Fructose stimulated colonic arginine and proline metabolism dysbiosis, altered microbiota and aggravated intestinal barrier dysfunction in DSS-induced colitis rats. Nutrients 15.
Sun, W., et al., 2023. Ketogenic diet attenuates neuroinflammation and induces conversion of M1 microglia to M2 in an EAE model of multiple sclerosis by regulating the NF-κB/NLRP3 pathway and inhibiting HDAC3 and P2X7R activation. Food Funct. 14, 7247–7269.
Tejaswini, M.S.S.R., et al., 2022. A comprehensive review on integrative approach for sustainable management of plastic waste and its associated externalities. Sci. Total Environ. 825, 153973.
Turner, J.R., 2009. Intestinal mucosal barrier function in health and disease. Nat. Rev. Immunol. 9, 799–809.
Wagner, S., Reemtsma, T., 2019. Things we know and don't know about nanoplastic in the environment. Nat. Nanotechnol. 14, 300–301.
Wu, Z., et al., 2021. Gut microbiota from green tea polyphenol-dosed mice improves intestinal epithelial homeostasis and ameliorates experimental colitis. Microbiome 9, 184.
Xie, R., et al., 2024. Desulfovibrio vulgaris interacts with novel gut epithelial immune receptor LRRC19 and exacerbates colitis. Microbiome 12, 4.
Xie, X., et al., 2021. Pi-dan-jian-qing decoction ameliorates type 2 diabetes mellitus through regulating the gut microbiota and serum metabolism. Front. Cell. Infect. Microbiol. 11, 748872.
Xu, D., et al., 2023. Differently surface-labeled polystyrene nanoplastics at an environmentally relevant concentration induced Crohn's ileitis-like features via triggering intestinal epithelial cell necroptosis. Environ. Int. 176, 107968.
Yang, J., et al., 2023. Epigallocatechin-3-gallate ameliorates polystyrene microplastics-induced anxiety-like behavior in mice by modulating gut microbe homeostasis. Sci. Total Environ. 892, 164619.
Yang, J., et al., 2024. Polystyrene nanoplastics induce cardiotoxicity by upregulating HIPK2 and activating the P53 and TGF-β1/Smad3 pathways. J. Hazard Mater. 474, 134823.
Yi, S., et al., 2023. Concentrate supplementation improves cold-season environmental fitness of grazing yaks: responsive changes in the rumen microbiota and metabolome. Front. Microbiol. 14, 1247251.
Zeng, W., et al., 2024. Enteral nutrition promotes the remission of colitis by gut bacteria-mediated histidine biosynthesis. EBioMedicine 100, 104959.
Zhang, K., et al., 2023a. Gut microbiota participates in polystyrene microplastics-induced hepatic injuries by modulating the gut-liver Axis. ACS Nano 17, 15125–15145.
Zhang, K., et al., 2023b. Gut microbiota-derived short-chain fatty acids ameliorate methamphetamine-induced depression- and anxiety-like behaviors in a Sigmar-1 receptor-dependent manner. Acta Pharm. Sin. B 13, 4801–4822.
Zhang, Q., et al., 2024. Effects of modified-BHI medium on the growth and metabolites of Akkermansia muciniphila. Food Sci. Biotechnol. 33, 1921–1930.
Zhang, S.S., et al., 2022. TLR4-IN-C34 inhibits lipopolysaccharide-stimulated inflammatory responses via downregulating TLR4/MyD88/NF-κB/NLRP3 signaling pathway and reducing ROS generation in BV2 cells. Inflammation 45, 838–850.
Zhong, Y., et al., 2024. Revealing new insights: two-center evidence of microplastics in human vitreous humor and their implications for ocular health. Sci. Total Environ. 921, 171109.